STEM CELLS®

TISSUE-SPECIFIC STEM CELLS

LncRNA-OG Promotes the Osteogenic Differentiation of Bone Marrow-Derived Mesenchymal Stem Cells Under the Regulation of hnRNPK

SU'AN TANG,[a,b,*] ZHONGYU XIE,[a,c,*] PENG WANG,[a,c,*] JINTENG LI,[c] SHAN WANG,[c] WENJIE LIU,[c] MING LI,[c] XIAOHUA WU,[d] HONGJUN SU,[d] SHUIZHONG CEN,[c] GUIWEN YE,[c] GUAN ZHENG,[c] YANFENG WU,[d] HUIYONG SHEN [a,c]

[a]Department of Orthopedics, The Eighth Affiliated Hospital, Sun Yat-sen University, Shenzhen, People's Republic of China; [b]Department of Orthopedics, Zhujiang Hospital, Southern Medical University, Guangzhou, People's Republic of China; [c]Department of Orthopedics, Sun Yat-sen Memorial Hospital, Sun Yat-sen University, Guangzhou, People's Republic of China; [d]Center for Biotherapy, Sun Yat-sen Memorial Hospital, Sun Yat-sen University, Guangzhou, People's Republic of China

[*]Contributed equally.

Correspondence: Huiyong Shen, M.D., Department of Orthopedics, The Eighth Affiliated Hospital, Sun Yat-sen University, 3025# Shen Nan Road, Shenzhen, Guangdong 518033, People's Republic of China. Telephone: 86-139-2227-6368; e-mail: shenhuiy@mail.sysu.edu.cn; or Yanfeng Wu, M.D., Center for Biotherapy, Sun Yat-sen Memorial Hospital, Sun Yat-sen University, 107# Yan Jiang Road West, Guangzhou, Guangdong 510120, People's Republic of China. Telephone: 86-136-0904-0860; e-mail: wuyf@mail.sysu.edu.cn

Received May 6, 2018; accepted for publication October 9, 2018; first published online in STEM CELLS *EXPRESS* October 29, 2018.

http://dx.doi.org/10.1002/stem.2937

Key Words. Long noncoding RNA • Mesenchymal stem cells • Osteogenic differentiation • Heterogeneous nuclear ribonucleoprotein K

ABSTRACT

Bone marrow-derived mesenchymal stem cells (BM-MSCs) are the main source of osteoblasts in vivo and are widely used in stem cell therapy. Previously, we analyzed long noncoding RNA (lncRNA) expression profiles during BM-MSC osteogenesis, and further investigation is needed to elucidate how lncRNAs regulate BM-MSC osteogenesis. Herein, we used customized microarrays to determine lncRNA expression profiles in BM-MSCs on days 0 and 10 of osteogenic differentiation. In addition, we identified a novel osteogenesis-associated lncRNA (lncRNA-OG) that is upregulated during this process. Functional assays showed that lncRNA-OG significantly promotes BM-MSC osteogenesis. Mechanistically, lncRNA-OG interacts with heterogeneous nuclear ribonucleoprotein K (hnRNPK) protein to regulate bone morphogenetic protein signaling pathway activation. Surprisingly, hnRNPK positively regulates lncRNA-OG transcriptional activity by promoting H3K27 acetylation of the lncRNA-OG promoter. Therefore, our study revealed a novel lncRNA with a positive function on BM-MSC osteogenic differentiation and proposed a new interaction between hnRNPK and lncRNA. STEM CELLS *2019;37:270–283*

SIGNIFICANCE STATEMENT

LncRNAs, previously thought to be transcriptional junk, have been proved to have significant functions on multiple biologic processes, especially in cell differentiation. Using customized microarrays to detect lncRNAs during the osteogenic differentiation of BM-MSCs, 1,050 differentially regulated lncRNAs were identified. Of 318 lncRNAs that were highly upregulated on day 10 of osteogenic differentiation, this study unveiled a novel positive functional osteogenesis-associated lncRNA, lncRNA-OG, which regulated the activation of BMP signaling pathway by interacting with hnRNPK. Furthermore, hnRNPK was demonstrated to positively regulate lncRNA-OG transcriptional activity. Study of osteogensis-associated lncRNA reveals a potential and valuable target in the process of BM-MSC osteogenesis for future clinical applications, and provides new insight into the relationship between hnRNPK and lncRNA.

INTRODUCTION

Bone formation is a complex process consisting of intramembranous ossification and endochondral ossification [1]. Mesenchymal stem cells (MSCs), harboring the self-renewal capability characteristic of human adult stem cells, can differentiate into osteoblasts in a process that generally accounts for intramembranous ossification [2]. Importantly, the osteogenic differentiation of bone marrow (BM)-derived MSCs has been widely applied in clinical practice, such as fracture healing of large bones and bone-related tissue engineering [3]. In addition, abnormal osteogenic differentiation of BM-MSCs is associated with a variety of diseases. Previous studies have shown that this process may play a vital role in the onset and development of ankylosing spondylitis (AS) and osteoarthritis (OA) [4, 5]. Therefore, further clarification of the molecular mechanism of MSC osteogenesis has become significantly important in studying bone disease as well as for clinical practice.

Long noncoding RNAs (lncRNAs) are an important type of RNA transcript that was recently

discovered and are longer than 200 nucleotides without protein-coding potential [6]. An increasing number of studies has shown that lncRNAs mediate gene expression *in cis* or *in trans*, thereby exerting crucial functions to regulate many biological processes, such as embryonic development, organ formation, and cell differentiation [7–10]. Previously, we analyzed lncRNA expression profiles during BM-MSC osteogenic differentiation [11]. However, the mechanism underlying lncRNA regulation of BM-MSC osteogenic differentiation remains largely unknown.

Heterogeneous nuclear ribonucleoprotein K (hnRNPK) is a member of the heterogeneous nuclear ribonucleoprotein (hnRNP) protein family [12]. As an evolutionarily conserved protein, hnRNPK participates in the regulation of many cellular processes, such as mRNA transcription, mRNA splicing, and chromatin remodeling [13]. Recent evidence has shown that hnRNPK and other members of the hnRNP family interact with multiple lncRNAs to regulate the expression of various genes [14–16]. However, the relationship between hnRNPK and lncRNAs and the functions of both molecules in BM-MSCs still need to be clarified.

In this study, we investigated the roles of lncRNAs in regulating of BM-MSC osteogenesis. We identified an evolutionarily conserved lncRNA expressed during BM-MSC osteogenic differentiation, which we termed osteogenesis-associated lncRNA (lncRNA-OG, gene symbol RP11-54A9.1). We found that lncRNA-OG is highly transcribed to promote BM-MSC osteogenesis. Mechanistically, we revealed that lncRNA-OG interacts with hnRNPK to regulate the expression of bone morphogenetic protein (BMP) family proteins. Surprisingly, we demonstrated that hnRNPK promotes lncRNA-OG transcriptional activity by regulating H3K27 acetylation of the lncRNA-OG promoter. Thus, our study found a novel lncRNA that functions in MSC osteogenesis, providing knowledge for the clinical application of MSCs and new insight into the relationship between hnRNPK and lncRNA.

Materials and Methods

Cell Isolation and Culture

This study was approved by the ethics committee of Sun Yat-sen Memorial Hospital (Guangzhou, People's Republic of China). After the possible risks and complications of bone marrow aspiration were explained, 15 healthy donors signed the informed consent form. BM-MSCs were isolated and cultured as previously described [4]. Generally, BM-MSCs were separated from bone marrow by density gradient centrifugation. Dulbecco's modified Eagle's medium (DMEM; Gibco, Waltham, MA) with 10% fetal bovine serum (FBS; Sijiqing, Hangzhou, People's Republic of China) was used to resuspend cells. In addition, cells were seeded into flasks and cultured in an incubator at 37°C, 5% CO_2 and 100% relative humidity. After 48 hours, the fluid was changed to remove suspended cells. Thereafter, the medium was changed every 3 days. When BM-MSCs reached 80%–90% confluence, 0.25% trypsin containing 0.53 mM EDTA was used to digest the cells. In addition, cells were evenly divided and reseeded into new flasks as passage 1. BM-MSCs were then expanded and used for in vitro and in vivo experiments at passages 3–5. In this study, all in vitro experiments were repeated thrice with three different BM-MSC donors.

BM-MSC Identification

To identify BM-MSC surface markers, the cells were digested and incubated with specific antibodies. The antibodies for surface markers were human CD14-PE, CD45-FITC, HLA-DR-PE, CD29-PE, CD44-FITC, and CD105-FITC (all from BD, San Jose, CA). A BD Influx cell sorter (BD) was used to perform flow cytometry.

For trilineage differentiation potential assays, BM-MSCs were cultured as we described previously [17]. For osteogenic differentiation, BM-MSCs were cultured with osteogenic differentiation medium (OM) consisting of DMEM with 10% FBS, 100 IU/ml penicillin, 100 IU/ml streptomycin, 0.1 μM dexamethasone, 10 mM β-glycerol phosphate, and 50 μM ascorbic acid (all from Sigma–Aldrich, St. Louis, MO). The medium was changed every 3 days. On day 14 of induction, alizarin red S (ARS) Staining (described below) was used to determine the osteogenic differentiation potential.

For adipogenic differentiation, BM-MSCs were cultured with adipogenic differentiation medium consisting of DMEM with 10% FBS, 10 μg/ml insulin (Sigma–Aldrich), 1 μM dexamethasone, 0.5 mM 3-isobutyl-1-methylxanthine (Sigma–Aldrich) and 0.2 mM indomethacin (Sigma–Aldrich). The medium was replaced every 3 days. On day 14 of induction, cells were fixed with 4% paraformaldehyde and stained with Oil Red O to detect the adipogenic differentiation potential.

For chondrogenic differentiation, approximately 5×10^5 cells were first centrifuged at 600*g* for 5 minutes to form pellets. Then, the cell pellets were cultured in chondrogenic differentiation medium consisting of high-glucose DMEM with 1% ITS-Premix (Corning, NY), 100 IU/ml penicillin, 100 IU/ml streptomycin, 50 μM ascorbic acid, 1 mM sodium pyruvate (Sigma–Aldrich), 0.1 μM dexamethasone, and 10 ng/ml recombinant human transforming growth factor-β3 (R&D Systems, Minneapolis, MN). On day 21 of induction, the cell pellets were fixed with 4% paraformaldehyde and embedded in paraffin. Alcian Blue staining was used to detect the chondrogenic differentiation potential.

Microarray

The detailed procedure for microarray analysis was performed as we described previously [11]. Briefly, total RNA was extracted from BM-MSCs with TRIzol (Thermo Fisher Scientific, Rockford, IL) on days 0 and 10 of osteogenic differentiation. RNA from three different BM-MSC donors was acquired for each time point. cDNA was synthesized, labeled with fluorescent dye and hybridized with a lncRNA Human Gene Expression Microarray v4.0 (4 × 180 K; Capital Bio Co., Beijing, People's Republic of China). Thereafter, a G2565CA microarray scanner (Agilent Technologies, Palo Alto, CA) was used to scan the microarray. Data were analyzed with GeneSpring software (Agilent). The criteria for further analysis of differentially expressed genes were a fold change of >2.0 or <2.0 and a p value <.05. Heat maps representing different gene expression levels were generated using Cluster 3.0. The microarray data were deposited in the Gene Expression Omnibus (GEO) public database under the accession number GSE113359.

5′- and 3′-Rapid Amplification of Cloned cDNA Ends

Rapid amplification of cloned cDNA ends (RACE) was performed using the SMARTer RACE cDNA amplification kit (Clontech,

Mountain View, CA) according to the manufacturer's instructions. Briefly, total RNA was extracted from cells using TRIzol reagent (Takara Bio, Mountain View, CA). In addition, the first-strand cDNA needed for subsequent 3′- and 5′-RACE experiments was synthesized using the provided reagents. Corresponding PCR primers (Supporting Information Table S1) were designed to produce the terminal cDNA fragment, which was validated by sequencing.

RNA Fluorescence In Situ Hybridization and Immunofluorescence Microscopy

The RNA-Fluorescence In Situ Hybridization (FISH) procedure was performed according to the detailed protocol from Biosearch Technologies (https://www.biosearchtech.com; Petaluma, CA). To detect lncRNA-OG RNA, Stellaris RNA-FISH probes against lncRNA-OG and all related reagents were purchased from Biosearch Technologies. Briefly, cells were rinsed in phosphate-buffered saline (PBS) and fixed in fixation buffer (3.7% formaldehyde solution with RNase-free PBS) for 10 minutes at room temperature. Then, cells were incubated with 0.1% Triton X-100 in PBS on ice for 5 minutes. Fluorescence-conjugated lncRNA-OG probes were used to perform hybridization in the dark at 37°C for at least 4 hours. For colocalization studies, after RNA-FISH, antibodies were added to detect RNA and protein colocalization. Laser scanning confocal microscopy (Carl Zeiss, Jena, Germany) was used to visualize the samples described above.

Reverse Transcription and Quantitative Real-Time Polymerase Chain Reaction

Total cellular RNA was isolated using TRIzol (Takara Bio) and used for first-strand cDNA synthesis with the PrimeScript RT reagent kit (Takara Bio). Quantification of all gene transcripts was performed by quantitative real-time polymerase chain reaction (qRT-PCR) using SYBR Premix Ex Taq (Takara Bio) according to the manufacturer's instructions on a 7,500 Real-Time PCR detection system (Applied Biosystems, Carlsbad, CA). Data were normalized to GAPDH or 18S expression in control samples. Primers for each gene are listed in Supporting Information Table S2.

Cell Cytoplasm/Nucleus Fractionation and Isolation

The PARIS kit (Thermo Fisher Scientific) was used to extract cytoplasmic and nuclear RNA from BM-MSCs according to the manufacturer's instructions. RNA extracted from each of the fractions was evaluated by qRT-PCR. Data were analyzed to evaluate the percentages of nuclear and cytoplasmic RNA.

RNA Interference and Transient Infection

Negative control (NC) and custom-made locked nucleic acid (LNA) GapmeR molecules targeting lncRNA-OG were purchased from Exiqon (Vedbaek, Denmark). Small interfering RNAs (siRNAs) targeting hnRNPK and NC were purchased from GenePharma (Suzhou, People's Republic of China). The sequences are listed in Supporting Information Table S3. According to the transient infection procedure, cells grown to 70%–90% confluence were transfected with siRNAs or LNAs using Lipofectamine RNAiMAX (Thermo Fisher Scientific). In addition, after 48 hours, cells were harvested to analyze RNA and protein expression. For osteogenic differentiation, cells were cultured in OM and harvested at days 7 and 14.

Lentivirus Infection

The detailed procedure for lentivirus infection was performed as we described previously [4]. Briefly, lncRNA-OG and hnRNPK overexpression lentiviruses (1×10^8 transfection units [TU]/ml) and a vector control (1×10^8 TU/ml) were purchased from GenePharma. Lentiviruses encoding short hairpin RNAs (shRNA) for hnRNPK were constructed with a target sequence of 5′-GGGTTGTAGAGTGCATAAA-3′. In addition, the sequence for the NC shRNA was 5′-TTCTCCGAACGTGTCACGTTTC-3′ (sh-NC). These two recombinant lentiviruses (1×10^9 TU/ml) were also purchased from GenePharma. All lentiviruses were used for BM-MSC infection at a multiplicity of infection of 50. Polybrene (5 mg/ml) was added to the lentivirus medium. In addition, the medium was replaced after 24 hours. To assess transduction efficiency, an inverted fluorescence microscope (Nikon, Tokyo, Japan) was used to calculate the percentage of GFP-positive cells.

Western Blotting

Cultured cells were harvested, washed with cold PBS, and lysed in RIPA buffer (Beyotime, Jiangsu, People's Republic of China) containing 1% PMSF (Sigma–Aldrich). Primary antibodies against RUNX2 (8486; Cell Signaling Technology [CST], Danvers, MA), total β-catenin (8480; CST), active β-catenin (19807; CST), ERK1/2 (4695; CST), phospho-ERK1/2 (4370; CST), hnRNPK (ab39975; Abcam, Cambridge, U.K.), smad1 (6944; CST), phospho-smad1/5/8 (13820; CST), BMP2 (ab14933; Abcam), BMP4 (ab124715; Abcam), BMP6 (ab155963; Abcam), BMP7 (ab129156; Abcam), BMP9 (ab207318; Abcam), β-actin (3700; CST), and GAPDH (ab8245; Abcam) were diluted 1:1,000 and incubated with the membranes at 4°C overnight. Horseradish peroxidase (HRP)-conjugated anti-rabbit IgG (Beyotime) or anti-mouse IgG (Beyotime) was diluted 1:1,000 and incubated with the membranes at room temperature for 1 hour. Immobilon Western chemiluminescent HRP substrate (Millipore, Billerica, MA) was used to visualize the membranes. ImageJ software (National Institutes of Health, Bethesda, MD) was used to quantify band intensities. The intensity of each band was normalized to that of GAPDH.

Alkaline Phosphatase Activity and Staining

To determine alkaline phosphatase (ALP) activity and staining, cells were cultured in OM for 7 days. ALP activity in cells was detected using an ALP assay kit (Nanjing Jiancheng Bioengineering Institute, Nanjing, People's Republic of China). A Pierce BCA protein assay kit (Thermo Fisher Scientific) was used to detect the total protein concentration. ALP activity in each sample was measured as units per gram of protein per 15 minutes. For ALP staining assays, the BCIP/NBT Alkaline Phosphatase Color Development Kit (Beyotime) was used according to the manufacturer's instructions.

ARS Staining and Quantification

For ARS staining and quantification, cells were cultured in OM for 14 days. First, BM-MSCs were fixed in 4% paraformaldehyde and then stained with 1% ARS (pH 4.3) for 15 minutes at room temperature. To remove nonspecific staining, the stained cells were washed thrice with PBS. Subsequently, the stained cells were observed under a microscope and photographed. For ARS quantification, 10% cetylpyridinium chloride monohydrate (Sigma–Aldrich)

was used to destain the cells for 1 hour at room temperature. Thereafter, 200 μl of liquid was transferred to a 96-well plate, and spectrophotometric absorbance was measured at 562 nm.

Bone Formation Assay In Vivo

This study was approved by the Animal Ethical and Welfare Committee of Sun Yat-Sen Memorial Hospital, Sun Yat-Sen University, Guangzhou, People's Republic of China. Bone formation assays in vivo were performed as described in our pervious study [18]. Briefly, BM-MSCs at the fourth passage infected with lentivirus (lncRNA-OG or NC) were cultured in OM for 7 days before the in vivo study. Cells were incubated with hydroxyapatite and β-tricalcium phosphate (HA/β-TCP, the National Engineering Research Center for Biomaterials of Sichuan University, Chengdu, People's Republic of China) scaffolds for 1 hour at 37°C, followed by centrifugation at 1,500 rpm for 5 minutes, then implanted into the dorsal side of 8-week-old BALB/c-nu/nu female mice (Laboratory Animal Center of Sun Yat-Sen University, Guangzhou, People's Republic of China). The mice were sacrificed, and the implants were obtained at 8 weeks. The implants obtained in the bone formation assay were successively fixed in 4% paraformaldehyde, decalcified in 10% EDTA (pH 7.4) for 2 weeks, embedded in paraffin and sliced into sections (5 μm thickness).

Hematoxylin and Eosin, Masson Trichrome and Immunohistochemical Staining

The sections were deparaffinized and hydrated. For Hematoxylin and Eosin (H&E) staining, sections were incubated with hematoxylin for 5 minutes. The sections were cleared in 1% HCl in 70% alcohol and further stained with eosin for 3 minutes. For Masson trichrome staining, the sections were stained using a Masson trichrome staining kit (Sigma–Aldrich) according to the manufacturer's protocol. Immunohistochemical staining was performed with a primary antibody against OCN (ab13420; Abcam) to investigate osteogenesis. All sections were visualized under a light microscope (Nikon).

RNA Pull-Down and Mass Spectrometry Assays

For RNA pull-down assays, biotin-labeled lncRNA-OG transcripts and antisense transcripts were obtained using in vitro transcription with T7 RNA polymerase from the TranscriptAid T7 High Yield Transcription Kit (Thermo Fisher Scientific) and purified with the Thermo GeneJET RNA Purification Kit (Thermo Fisher Scientific). Biotinylated RNA was incubated with BM-MSC nuclear extracts according to the manufacturer's instructions for the Pierce Magnetic RNA-Protein Pull-down Kit (Thermo Fisher Scientific). SDS-PAGE was used to separate the pull-down proteins, and silver staining was subsequently performed using Pierce Silver Stain for Mass Spectrometry (Thermo Fisher Scientific). Differential bands specifically enriched by lncRNA-OG were collected for mass spectrometry.

RNA Immunoprecipitation

RNA immunoprecipitation (RIP) was performed using the Magna Nuclear RIP (Native) Nuclear RNA-Binding Protein Immunoprecipitation Kit (Millipore) according to the manufacturer's instructions. Briefly, for concentrated nuclear lysates, an appropriate, quantified number of cells was lysed with RIP lysis buffer containing protease inhibitor cocktail and RNase inhibitor (provided by the kit). Magnetic beads were incubated with antibodies against hnRNPK (ab39975; Abcam) or NC mouse IgG (provided by the kit). Thereafter, different bead-antibody complexes were immunoprecipitated from cell lysates. Precipitated RNAs was isolated with TRIzol and subsequently analyzed by qRT-PCR. Data were normalized to the input control.

Chromatin Immunoprecipitation

Chromatin immunoprecipitation (ChIP) assays were performed using the EZ-Magna ChIP A/G Assay kit (Millipore) according to the manufacturer's instructions. Briefly, cells were crosslinked with 1% formaldehyde at room temperature for 10 minutes. Then, cells were collected and lysed to isolate the nuclei with nuclear lysis buffer containing protease inhibitor cocktail (provided by the kit). Sonication was performed to shear chromatin, generating 200–1,000-bp DNA fragments. The sheared chromatin was immunoprecipitated with primary antibodies, such as hnRNPK (ab39975; Abcam), histone H3 lysine 27 acetylation (H3K27ac; ab39975; Abcam), normal mouse IgG and anti-RNA polymerase II antibody (provided by the kit). After protein-DNA crosslinking was reversed, the precipitated DNA was purified and subsequently analyzed by qRT-PCR. Data were normalized to the input control. The ChIP-qPCR primers used are listed in Supporting Information Table S4.

Statistical Analysis

Data were analyzed using GraphPad Prism 7 (GraphPad, La Jolla, CA). All data are expressed as the mean ± SD of three independent experiments. Student's *t* test or one-way analysis of variance was used to determine the differences between two groups. *p* values of less than .05 were considered statistically significant.

Results

Phenotype Identification and Trilineage Differentiation Potential of BM-MSCs

To characterize cultured cells, we used flow cytometry to detect their phenotype and conducted trilineage differentiation potential assays to determine their differentiation potential. The results suggested that the isolated BM-MSCs were negative for CD14, CD45, and HLA-DR and positive for CD29, CD44, and CD105 (Fig. 1A). In addition, these cells successfully differentiated into osteoblasts, adipocytes, and chondroblasts (Fig. 1B). Therefore, in this study, isolated cells met the International Society for Stem Cell Research standard for MSC identification [19].

LncRNA-OG Is Upregulated during BM-MSC Osteogenic Differentiation

To investigate the roles of lncRNAs in the process of BM-MSC osteogenesis, customized microarrays were used to determine lncRNA expression profiles in BM-MSCs. Expression profiles were detected on days 0 and 10 of osteogenic differentiation. Analysis revealed that 1,050 annotated or potential lncRNAs were up- or downregulated by ≥2-fold during osteogenic differentiation (Student's *t* test, false discovery rate [FDR] < 0.2; Fig. 2A). Among them, 732 lncRNAs showed a decrease in expression, while the remaining lncRNAs (318) were highly upregulated on day 10 of osteogenic differentiation. Among these lncRNAs, we identified a lncRNA that was upregulated by almost 12-fold, which we termed

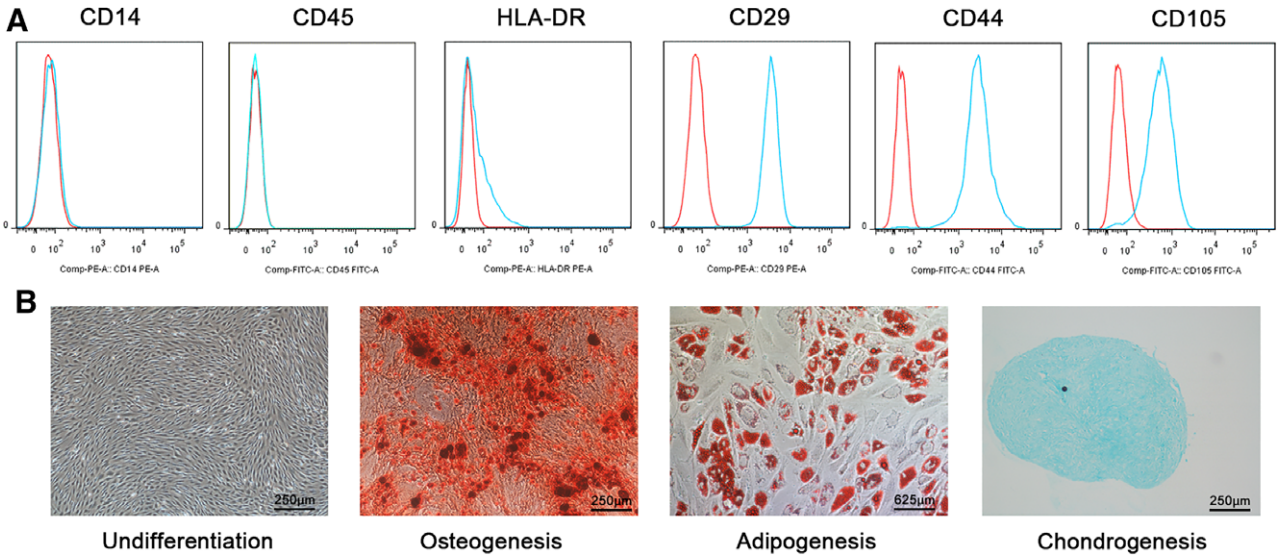

Figure 1. Phenotype identification and trilineage differentiation potential of bone marrow-derived mesenchymal stem cells (BM-MSCs). **(A):** BM-MSCs were negative for CD14, CD45, and HLA-DR expression and positive for CD29, CD44, and CD105 expression. **(B):** BM-MSCs were induced to undergo osteogenic differentiation, adipogenic differentiation, and chondrogenic differentiation. Scale bars in undifferentiation, osteogenesis, and chondrogenesis, 250 μm. Scale bar in adipogenesis, 625 μm.

lncRNA-OG. qRT-PCR confirmed the significantly increased expression of lncRNA-OG at various time points during BM-MSC osteogenesis (Fig. 2B).

LncRNA-OG is located on human chromosome 12 between the NAP1L1 and BBS10 genes (Fig. 2C). Using 5′- and 3′-RACE, we further amplified the full-length lncRNA-OG and validated the results via sequencing (Supporting Information Fig. S1A). LncRNA-OG contains four exons, comprising 878 nucleotides, at a modestly conserved locus according to Phylop analysis (Fig. 2C). In addition, we used three different authoritative prediction algorithms—Coding Potential Calculator, Coding Potential Assessment Tool and PhyloCSF—to analyze the protein-coding potential of lncRNA-OG. These algorithms all suggested that lncRNA-OG did not harbor protein-coding potential, which was demonstrated by in vitro experiments (Supporting Information Fig. S1B, S1C). We also estimated the copy number of lncRNA-OG RNA molecules per BM-MSC cell during BM-MSC osteogenesis by absolute quantitative PCR (Supporting Information Fig. S1D and Table S5). According to RNA-FISH results, we found that lncRNA-OG was mainly located in the nucleus of BM-MSCs (Fig. 2D), which was confirmed by nuclear/cytoplasm fractionation (Fig. 2E). These results indicated that lncRNA-OG may exert its biological function in the nucleus.

LncRNA-OG Promotes the Osteogenic Differentiation of BM-MSCs

We next determined the functional role of lncRNA-OG during BM-MSC osteogenesis. We used LNA GapmeR molecules to silence lncRNA-OG and lentivirus infection to overexpress lncRNA-OG transcripts on day 0, followed by culture in OM. To control potential off-target effects, we designed three LNA candidates targeting lncRNA-OG and selected the two most efficient LNAs (termed LNA-1, against exon 1, and LNA-2, against exon 4) for subsequent experiments. To assess experimental reliability, we confirmed that lncRNA-OG expression decreased by over 50% with the application of LNAs and increased by almost 12-fold in the overexpression group compared with the control group (Supporting Information Fig. S2A). LncRNA-OG knockdown significantly delayed the osteogenic differentiation of BM-MSCs, as shown by the visualization and quantification of ALP and ARS staining, while lncRNA-OG overexpression promoted osteogenic differentiation (Fig. 3A). Consistently, the expression of osteogenic markers, including *RUNX2*, *ALP*, osterix (*OSX*), and osteocalcin (*OCN*), was markedly reduced in lncRNA-OG-knockdown cells compared with the control group, while lncRNA-OG overexpression induced the opposite effect (Fig. 3B and Supporting Information Fig. S2C). Moreover, Western blotting showed that RUNX2 protein levels were decreased in the lncRNA-OG knockdown group and increased in the lncRNA-OG overexpression group on day 7 of osteogenic differentiation (Fig. 3C).

To demonstrate the effect of lncRNA-OG on osteogenesis, BM-MSCs were infected with lncRNA-OG overexpression lentivirus and NC for 7 days in vitro. After that, cells were loaded onto scaffolds and implanted in the subcutaneous space of nude mice (five mice per group). After 8 weeks, the implantation samples were harvested and subjected to assess the osteogenesis in vivo. H&E staining revealed little newly formed bone in the NC group, while osteoid was formed in the lncRNA-OG overexpression group (Fig. 3D). Collagen organization with blue color in Masson's trichrome staining was significantly higher in the lncRNA-OG overexpression group (Fig. 3D). Additionally, immunohistochemical staining for OCN indicated that both the range and intensity of the stained granules in osteoblasts were generally increased in the lncRNA-OG overexpression group (Fig. 3D). Together, these data indicate that lncRNA-OG promotes BM-MSC osteogenic differentiation.

LncRNA-OG Associates with hnRNPK in BM-MSC Nuclei

Notably, lncRNA-OG is an internal lncRNA that may regulate the expression of its nearby genes *in cis.* However, we found that lncRNA-OG depletion did not affect nearby genes (Supporting Information Fig. S3A), suggesting that lncRNA-OG

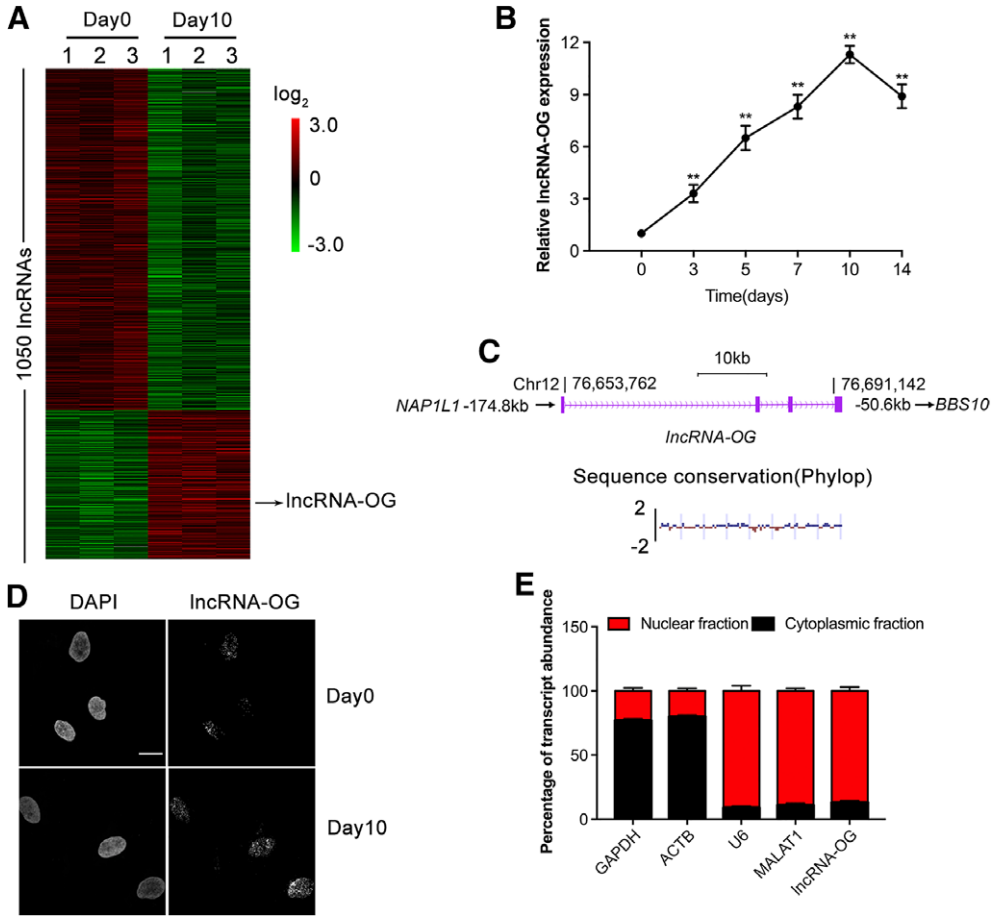

Figure 2. Osteogenesis-associated long noncoding RNA (lncRNA-OG) is highly expressed during bone marrow-derived mesenchymal stem cell (BM-MSC) osteogenesis. **(A):** Geometric mean-centered, hierarchical clustering heat map from microarray data. The 1,050 differentially (≥ 2-fold) expressed (two-tailed, paired Student's *t* test, and false discovery rate < 0.2) annotated noncoding RNAs ($p < .05$) on days 0 and 10 of osteogenic differentiation. Microarray data are from three independent biological replicates. **(B):** Relative expression of lncRNA-OG at various time points during BM-MSC osteogenic differentiation, as determined by quantitative real-time polymerase chain reaction (qRT-PCR). GAPDH was used for normalization. **(C):** Schematic annotation of the lncRNA-OG genomic locus on chromosome 12. Purple rectangles represent exons (upper panel). Sequence conservation was analyzed by Phylop software (lower panel). **(D):** LncRNA-OG intracellular localization was visualized in BM-MSCs by RNA-fluorescence in situ hybridization assays. Representative images of lncRNA-OG on days 0 and 10 of osteogenesis are shown. DAPI, 4′,6-diamidino-2-phenylindole. Probes, lncRNA-OG. Scale bar, 20 μm. **(E):** Percentages of nuclear and cytoplasmic RNA, as measured by qRT-PCR after subcellular MSC fractionation. GAPDH and ACTB RNA served as positive controls for cytoplasmic gene expression. U6 and MALAT1 RNA served as positive controls for nuclear gene expression. Data are presented as the mean ± SD. *, $p < .05$; **, $p < .01$ ($n = 3$ independent experiments). Data represent at least three independent experiments. See also Supporting Information Figure S1.

might exert its function *in trans.* To explore potential proteins associated with lncRNA-OG, we performed RNA pull-down assays with BM-MSC cell lysates and biotin-labeled lncRNA-OG. Silver staining revealed the appearance of two clearly different bands (Fig. 4A). Through mass spectrometry, we identified one specific protein as hnRNPK (Supporting Information Fig. S3B). We confirmed that lncRNA-OG precipitated with hnRNPK in BM-MSC cell lysates in RNA pull-down experiments (Fig. 4B). Furthermore, the interaction between lncRNA-OG and hnRNPK was validated by RIP (Fig. 4C). HnRNPK was mainly expressed in the nucleus of BM-MSCs (Supporting Information Fig. S3C), and upregulated during BM-MSCs osteogenesis (Supporting Information Fig. S3D). Moreover, lncRNA-OG colocalized with hnRNPK in the nucleus of BM-MSCs (Fig. 4D). To further determine the fragment of lncRNA-OG binding hnRNPK, we constructed a series of lncRNA-OG truncated fragments. We found that the 3′-end lncRNA-OG fragment (nt 645 to 878) was sufficient to bind hnRNPK (Fig. 4E). Furthermore, we predicted the structure of lncRNA-OG exon 4 by RNA folding analysis, which showed a stable stem-loop structure (Fig. 4F), indicating high binding affinity between lncRNA-OG and hnRNPK. These data show that lncRNA-OG associates with hnRNPK to form an RNA-protein complex in BM-MSC nuclei.

LncRNA-OG Regulates the Expression of BMP Family Proteins by Interacting with hnRNPK

Multiple signaling pathways, such as the WNT/β-catenin pathway, MAPK pathway and BMP/Smad1/5/8 pathway, are involved in the regulation of BM-MSC osteogenic differentiation [20]. Previously, we demonstrated that lncRNA-OG promoted the osteogenic differentiation of BM-MSCs in vitro. To determine which pathways lncRNA-OG specifically affects, we knocked down lncRNA-OG with LNA-1 and LNA-2 and overexpressed lncRNA-OG with lentivirus during osteogenesis. We detected the phosphorylation levels of Smad1/5/8 and ERK-1/2 and the expression of active β-catenin on day 7 of osteogenesis. The

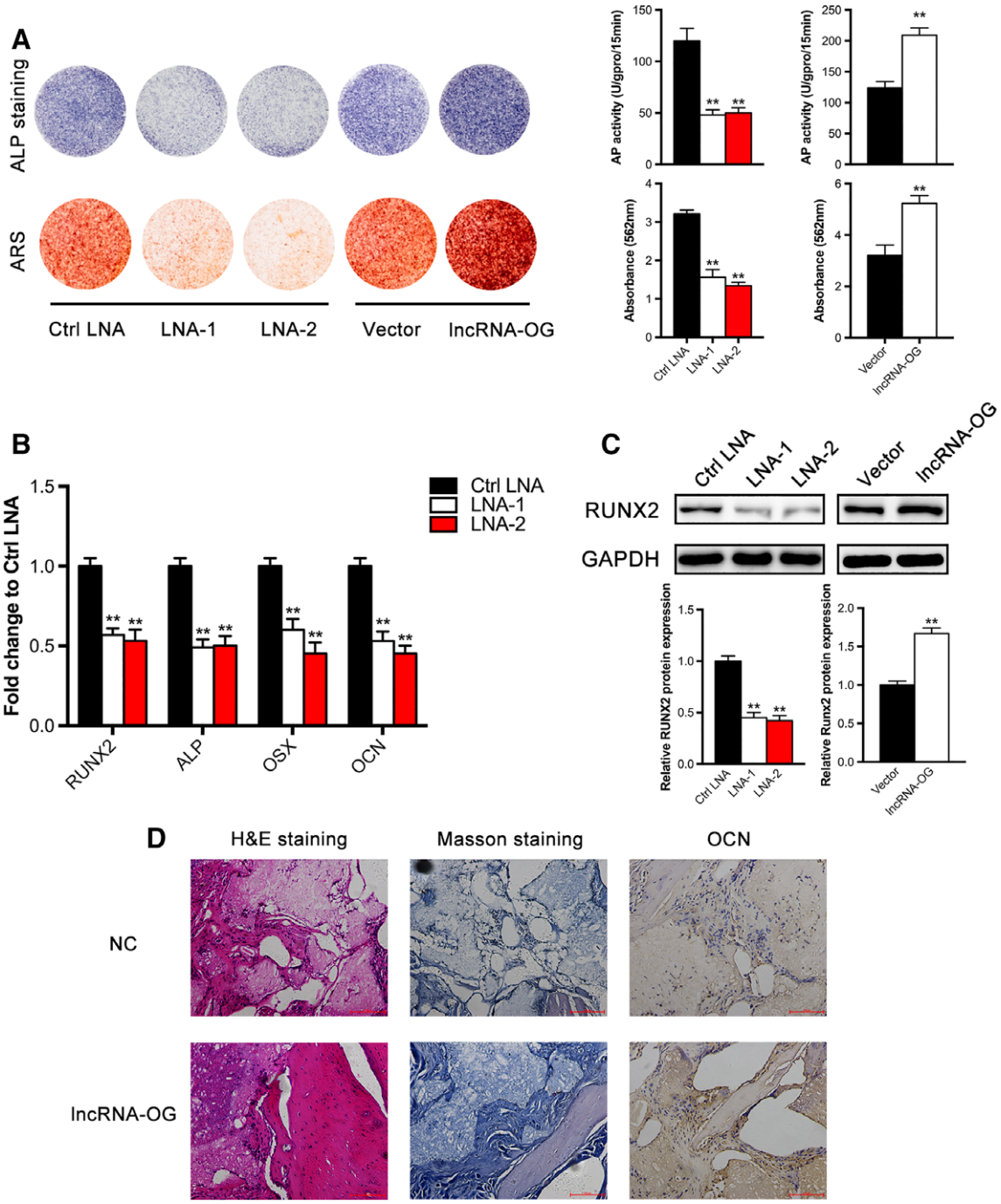

Figure 3. Osteogenesis-associated long noncoding RNA (lncRNA-OG) promotes the osteogenic differentiation of bone marrow-derived mesenchymal stem cells (BM-MSCs). **(A):** Left: alkaline phosphatase (ALP) staining on day 7 (upper panel), alizarin red (ARS) staining on day 14 after osteogenic induction (lower panel). Right: ALP activity was determined as units per gram of protein per 15 minutes. ARS staining was quantified as the absorbance at 562 nm. **(B):** Relative mRNA levels of *RUNX2* and *ALP* detected by quantitative real-time polymerase chain reaction (qRT-PCR) on day 7 of osteogenic differentiation. Relative mRNA levels of *OSX* and *OCN* detected by qRT-PCR on day 10 of osteogenic differentiation. Data were normalized to *GAPDH* expression. **(C):** Western blotting analysis of RUNX2 protein levels on day 7 of osteogenic induction. GAPDH was used as the internal control (upper panel). Lower, quantification of band intensities (lower panel). **(D):** H&E staining, Masson's trichrome staining, and immunohistochemical staining of OCN in lncRNA-OG and NC groups. Scale bars, 100 μm. Data are presented as the mean ± SD. *, $p < .05$; **, $p < .01$ ($n = 3$ independent experiments). See also Supporting Information Figure S2.

results revealed that lncRNA-OG remarkably affected Smad1/5/8 phosphorylation levels but had no significant effect on ERK1/2 phosphorylation or active β-catenin levels (Fig. 5A). Since lncRNA-OG mainly affected the BMP signaling pathway, we speculated whether lncRNA-OG regulated the expression of BMP family proteins. When we detected the expression of BMP family proteins, we found that *BMP-2*, *BMP-4*, and *BMP-6* gene expression decreased by varying degrees after lncRNA-OG

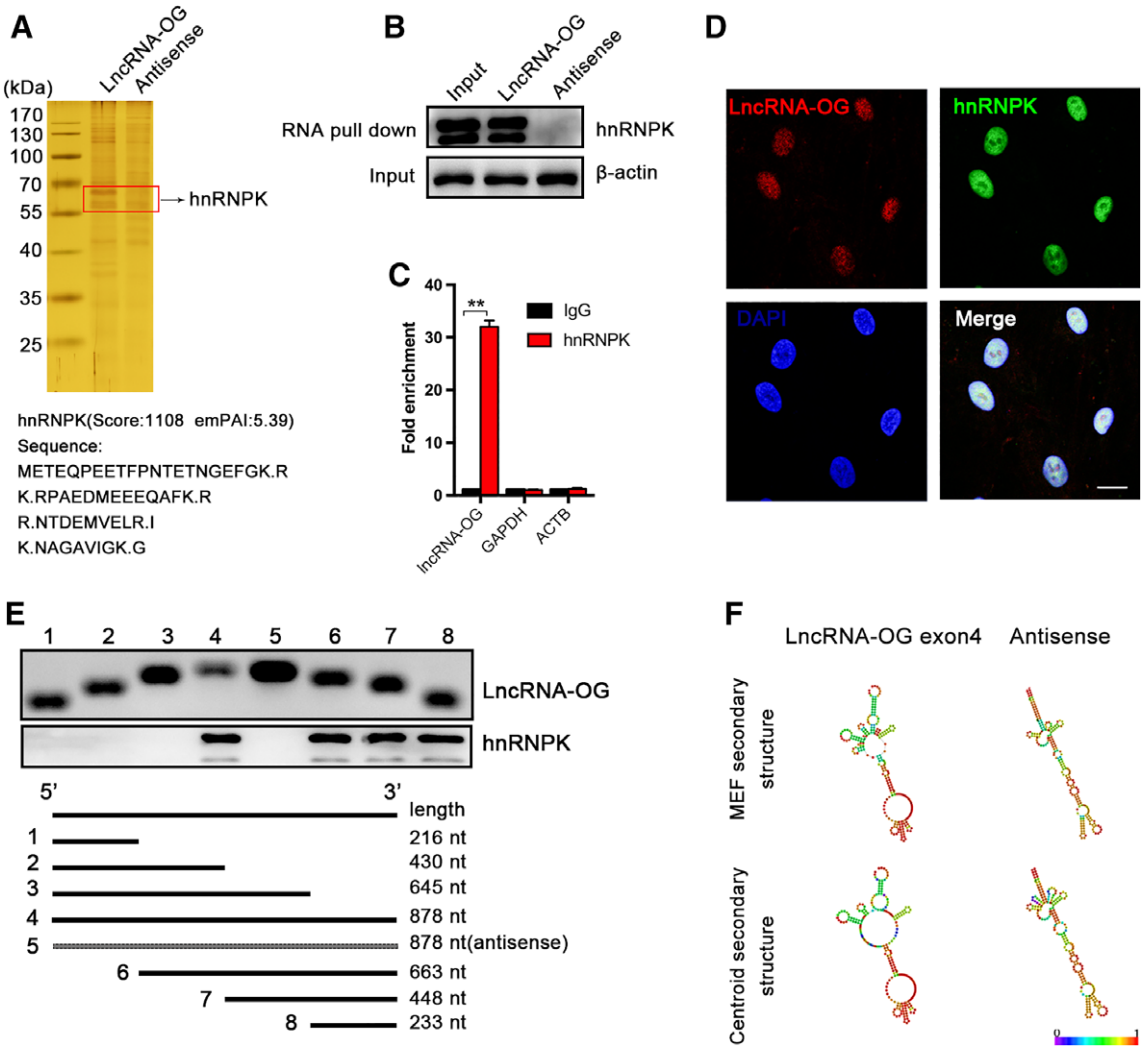

Figure 4. Osteogenesis-associated long noncoding RNA (lncRNA-OG) interacts with hnRNPK in the nuclei of bone marrow-derived mesenchymal stem cells (BM-MSCs). **(A):** Silver staining of RNA pull-down precipitates. Biotin-RNA pull-down assays were performed with MSC nuclear extracts using full-length lncRNA-OG transcripts and lncRNA-OG reverse-complement transcripts (antisense). Pull-down assays were followed by mass spectrometry. **(B):** Western blotting analysis of the specific association between hnRNPK and lncRNA-OG. β-Actin was used as a control. **(C):** The interaction between lncRNA-OG and hnRNPK was verified by RIP assays. **(D):** Colocalization of lncRNA-OG and hnRNPK in MSC nuclei. Scale bars, 20 μm. **(E):** In vitro-transcribed biotin-labeled RNA (top panel); associated hnRNPK was detected by Western blotting analysis (middle panel); schematic diagram of full-length lncRNA-OG and truncated fragments (bottom panel). **(F):** Exon 4 (nucleotides 645–878) of lncRNA-OG was predicted to have a stable stem-loop structure. Prediction of the exon 4 region of the lncRNA-OG structure and its antisense sequence was based on minimum free energy and the partition function. The color scale shows the confidence of the prediction for each base, with shades of red indicating strong confidence (http://rna.tbi.univie.ac.at). Data are shown as the mean ± SD. **, $p < .01$ ($n = 3$ independent experiments). See also Supporting Information Figure S3.

knockdown (Fig. 5B, 5C). To further clarify whether hnRNPK was involved in regulating the osteogenic differentiation of BM-MSCs, we designed two siRNAs (si-hnRNPK-1 and si-hnRNPK-2) that efficiently interfere with hnRNPK (Supporting Information Fig. S4A). HnRNPK knockdown significantly delayed BM-MSC osteogenesis (Supporting Information Fig. S4B) and abrogated the positive effects of lncRNA-OG on BM-MSC osteogenic differentiation (Fig. 5D). This result indicated that hnRNPK plays an important role in the function of lncRNA-OG. Furthermore, experiments showed that *BMP-2*, *BMP-4*, *BMP-6*, *BMP-7*, and *BMP-9* decreased after hnRNPK knockdown (Fig. 5C and Supporting Information Fig. S4C). Moreover, the promotion effect of lncRNA-OG and hnRNPK on BMP family proteins were demonstrated by overexpression of lncRNA-OG and hnRNPK, respectively (Supporting Information Fig. S4D). Together, these results suggest that lncRNA-OG may regulate the expression of BMP family proteins to promote osteogenic differentiation by interacting with hnRNPK.

HnRNPK Promotes lncRNA-OG Transcription

To investigate whether there is a regulatory relationship between hnRNPK and lncRNA-OG, we performed siRNA-mediated hnRNPK knockdown. To our surprise, we found that lncRNA-OG was substantially downregulated (Fig. 6A). Interestingly, hnRNPK expression was not substantially affected after lncRNA-OG depletion (Fig. 6B, 6C). Based on these results, we next determined whether hnRNPK regulated lncRNA-OG synthesis or degradation. To further investigate this question, we

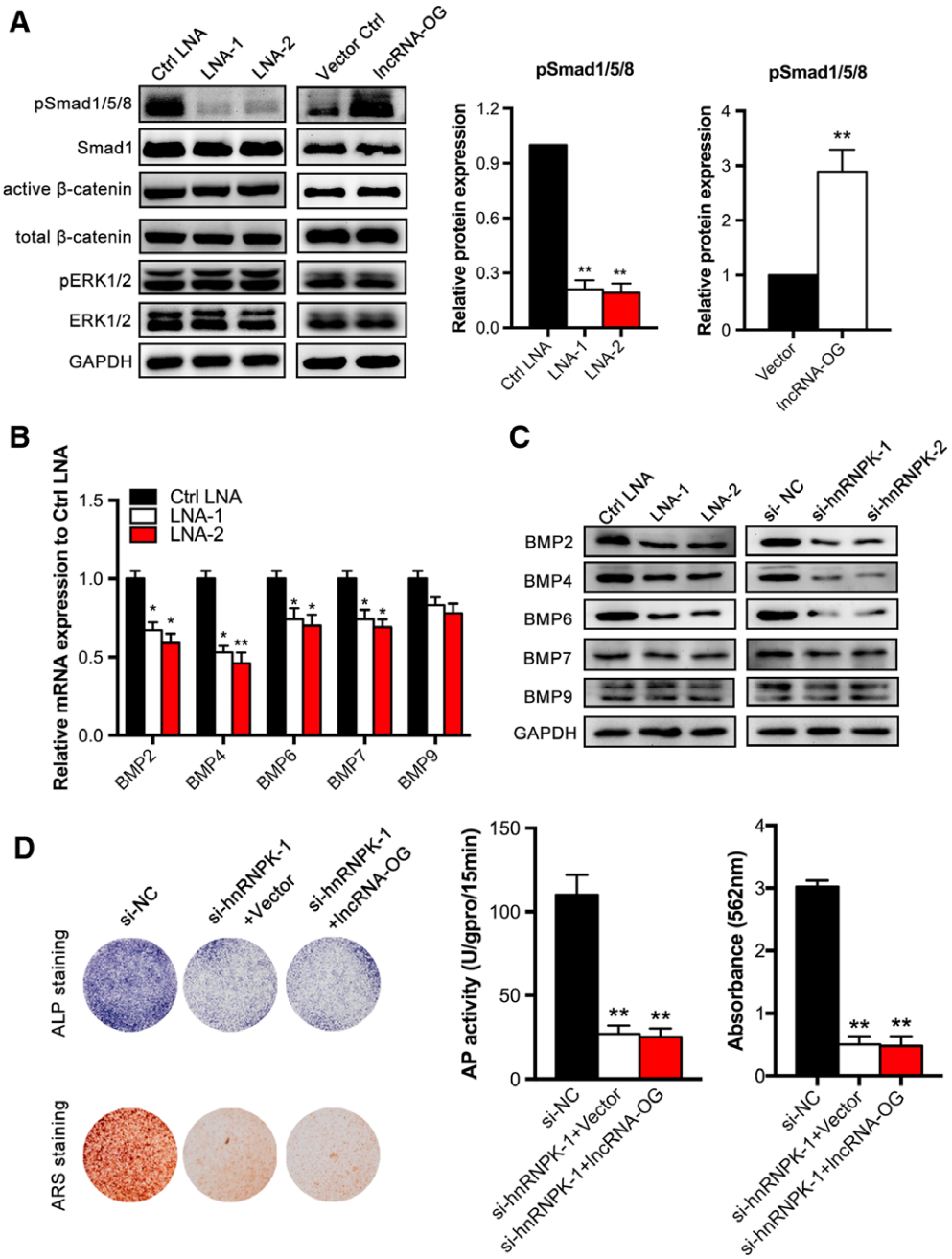

Figure 5. Osteogenesis-associated long noncoding RNA (lncRNA-OG) regulates the expression of bone morphogenetic protein (BMP) family proteins by interacting with hnRNPK. **(A):** Expression analysis of BMP signaling, β-catenin/WNT signaling and ERK1/2/MAPK signaling following lncRNA-OG knockdown and overexpression in bone marrow-derived mesenchymal stem cells (BM-MSCs) by Western blotting. GAPDH was used as the internal control (left panel). Quantification of pSmad1/5/8 band intensities (right panel). **(B):** Related mRNA levels of *BMP2*, *BMP4*, *BMP6*, *BMP7*, and *BMP9* after lncRNA-OG knockdown on day 7 of osteogenic differentiation. Data were normalized to GAPDH. **(C):** Expression of BMP family proteins following lncRNA-OG and hnRNPK knockdown respectively in BM-MSCs by Western blotting. GAPDH was used as the internal control. **(D):** Left: alkaline phosphatase (ALP) staining on day 7 (upper panel), alizarin red (ARS) staining on day 14 after osteogenic induction (lower panel). Right: ALP activity was determined as units per gram of protein per 15 minutes. ARS staining was quantified as the absorbance at 562 nm. Data are presented as the mean ± SD. *, $p < .05$; **, $p < .01$ ($n = 3$ independent experiments). See also Supporting Information Figure S4.

enhanced or inhibited hnRNPK expression in BM-MSCs. In addition, we treated the cells with actinomycin D (ActD, 3 μg/ml) or dimethylsulfoxide (NC) over a 24-hour period to block new RNA synthesis and then measured the reduction in lncRNA-OG, GAPDH, and 18S RNA expression over different periods of time. By detecting changes in GAPDH expression after ActD stimulation, we determined that mRNA synthesis was successfully inhibited (Fig. 6D). Under these conditions, lncRNA-OG expression was not significantly downregulated after hnRNPK was silenced (Fig. 6E). Similarly, hnRNPK overexpression promoted the transcription of lncRNA-OG compared with that in the control group, while this effect disappeared

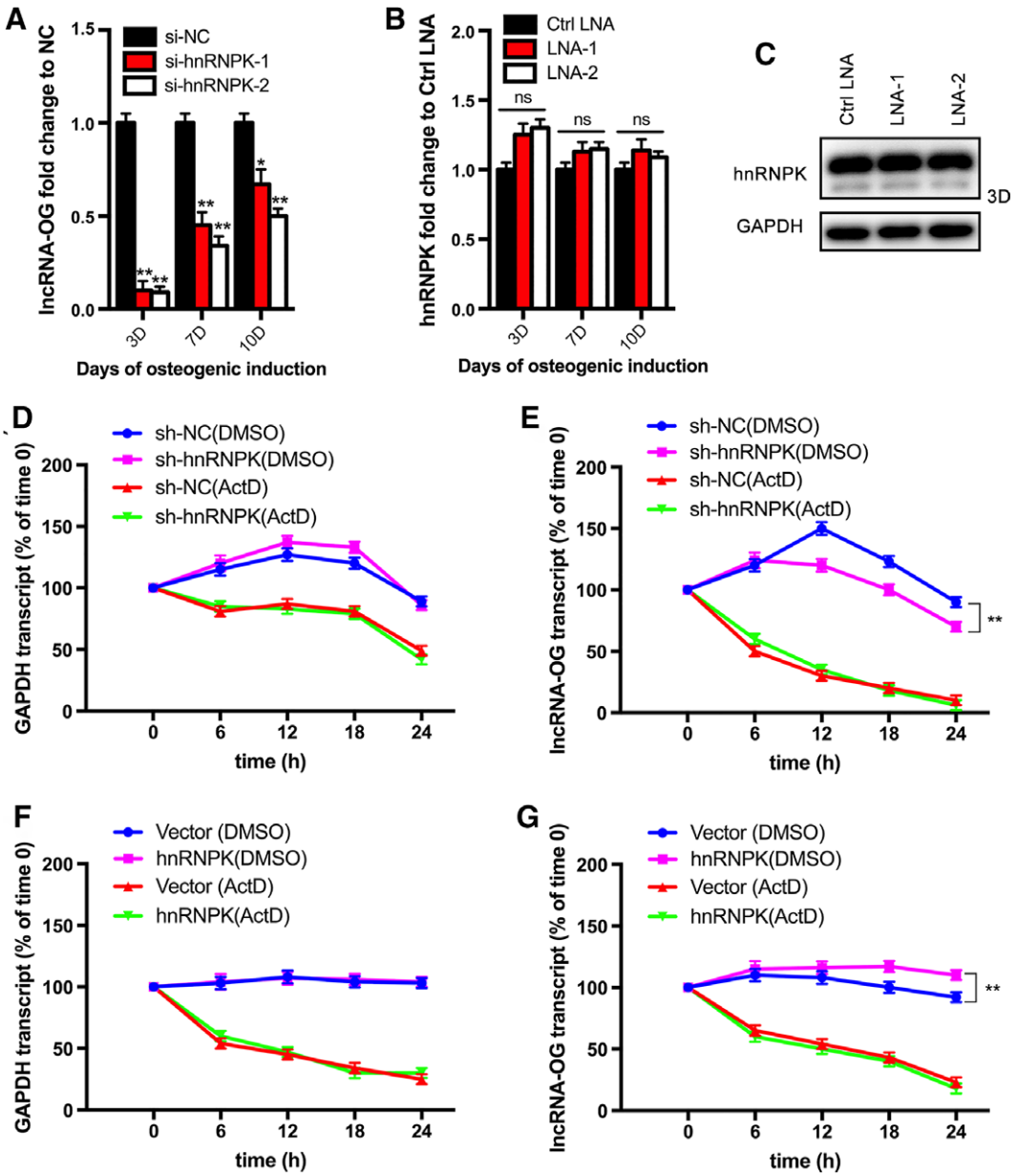

Figure 6. HnRNPK promotes osteogenesis-associated long noncoding RNA (lncRNA-OG) transcription. **(A):** Related expression of lncRNA-OG after hnRNPK knockdown on days 3, 7, and 10 of osteogenic differentiation. **(B):** Related mRNA levels of *hnRNPK* after lncRNA-OG knockdown on days 3, 7, and 10 of osteogenic differentiation. **(C):** Western blotting analysis of hnRNPK protein levels on day 3 of osteogenic differentiation after lncRNA-OG knockdown. **(D–G):** Related expression of GAPDH and lncRNA-OG transcripts after blocking new RNA synthesis using actinomycin D (ActD) or dimethylsulfoxide (negative control) and normalizing to 18S rRNA expression. (D) and (E) show the group with hnRNPK silenced. (F) and (G) show the group with hnRNPK overexpression. Data are presented as the mean ± SD. Ns > 0.05; *, $p < .05$; **, $p < .01$ ($n = 3$ independent experiments).

with ActD treatment (Fig. 6F, 6G). These results indicated that hnRNPK promotes lncRNA-OG transcription rather than its degradation.

HnRNPK Promotes lncRNA-OG Transcriptional Activity by Increasing H3K27ac

Previous studies have demonstrated that hnRNPK directly binds to the promoter regions of genes and participates in gene transcription regulation. Therefore, we reasoned that hnRNPK is involved in lncRNA-OG transcription based on the results described above. To validate it, we performed ChIP experiments with antibodies against hnRNPK. We designed six pairs of primers for the lncRNA-OG promoter region to obtain ChIP experimental results (Fig. 7A), which showed that hnRNPK directly bound to the primer 4 region (−754 to −523) in the lncRNA-OG promoter (Fig. 7B). Additionally, according to the University of California Santa Cruz (UCSC) Genome Bioinformatics Site (http://genome.ucsc.edu/), we found that H3K27ac was substantially enriched in the lncRNA-OG promoter region (Fig. 7A). ChIP assays confirmed that H3K27 acetylation occurred in the lncRNA-OG promoter during osteogenesis (Fig. 7B, 7C). To demonstrate that hnRNPK enhances lncRNA-OG promoter acetylation, we found that hnRNPK inhibition decreased H3K27ac levels in the lncRNA-OG promoter region (Fig. 7D), while hnRNPK

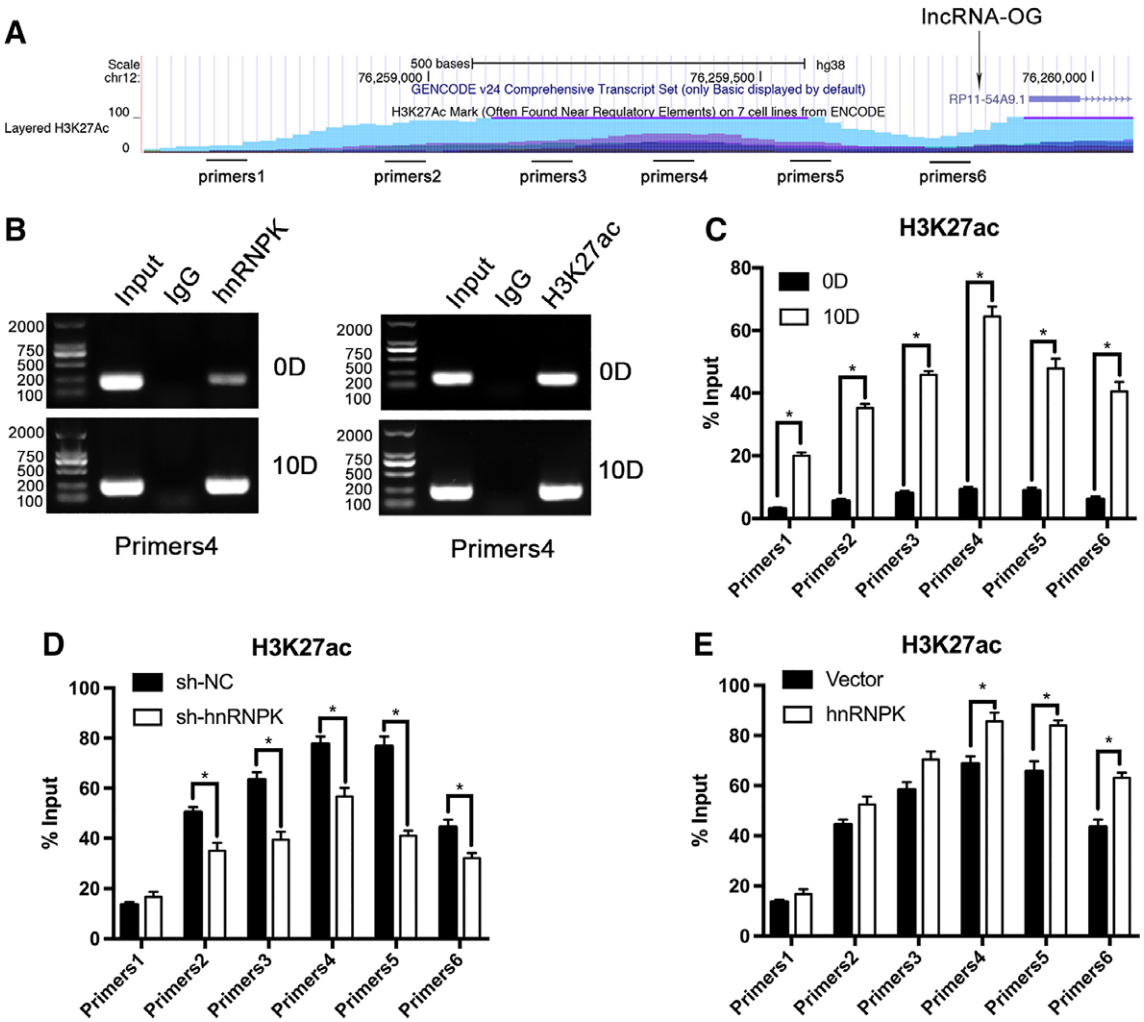

Figure 7. HnRNPK promotes osteogenesis-associated long noncoding RNA (lncRNA-OG) transcriptional activity by increasing H3K27ac. **(A):** Schematic diagram of the lncRNA-OG promoter region showing strong indications of histone H3 acetylation. Histone modification data were retrieved from the ENCODE collection. Six pairs of primers were designed for the promoter region. **(B):** Left: HnRNPK binding to the lncRNA-OG promoter region were assessed by ChIP using primers for exon 4 on days 0 and 10 of osteogenesis. Right: ChIP assay of H3K27ac in the lncRNA-OG promoter region using primers for exon 4 on days 0 and 10 of osteogenesis. **(C):** H3K27ac enrichment in the lncRNA-OG promoter region during osteogenic differentiation by ChIP-qPCR. ChIP-qPCR assay of H3K27ac in the lncRNA-OG promoter region using six pairs of primers after hnRNPK knockdown **(D)** and hnRNPK overexpression **(E)**. Data are presented as the mean ± SD. *, $p < .05$ ($n = 3$ independent experiments).

overexpression increased H3K27ac levels (Fig. 7E). These data suggest that hnRNPK increases promoter histone acetylation to promote lncRNA-OG transcriptional activity.

Discussion

In this study, we evaluated lncRNA expression profiles during the osteogenic differentiation of BM-MSCs and identified an upregulated transcript during BM-MSC osteogenesis termed lncRNA-OG. LncRNA-OG is a functional osteogenesis-associated lncRNA that significantly promotes BM-MSC differentiation into osteoblasts by regulating the expression of BMP family proteins via interactions with hnRNPK. Surprisingly, hnRNPK promotes lncRNA-OG transcriptional activity by affecting H3K27ac in the lncRNA-OG promoter.

MSCs, especially those from bone marrow, are pluripotent mesenchymal progenitors that serve as long-term precursors for the differentiation of a variety of cells, including osteoblasts, chondroblasts, and adipocytes [21]. Among these different types of differentiation, MSC osteogenic differentiation has been widely studied because of its crucial role in a variety of physiological and pathological processes. Studies have reported that MSCs have a high propensity toward osteogenesis in ossification of the posterior longitudinal ligament (OPLL) patients [22]. Similarly, subchondral MSCs isolated from patients with end-stage knee OA exhibited increased proliferative and osteogenic abilities [5]. Moreover, our previous study demonstrated that BM-MSCs from AS patients displayed an abnormally enhanced osteogenic differentiation capacity in vitro [4]. Therefore, it is necessary to study the regulatory mechanism of osteogenesis and to further clarify the specific functional molecules involved. In the experiments described above, MSCs were separated from human bone marrow and cultured in OM to induce osteogenesis. As MSC osteogenic differentiation is the main source of osteoblasts in vivo, studying the regulatory

mechanism underlying this process is helpful for identifying new targets and holds great value for clinical applications.

LncRNAs have been reported to play crucial roles in a variety of cellular processes. Notably, a considerable amount of research suggests that lncRNAs regulate stem cell differentiation, including RMST in neuronal differentiation [23], ADINR in adipocyte differentiation [24] and lncRNA-HIT in chondrocyte differentiation [25]. Previously, lncRNAs with potential roles in osteoblast differentiation have been identified, including H19, MEG3, lncRNA-MIR31HG, and lncRNA-POIR [26–29]. Although lncRNAs related to osteogenic differentiation have been studied previously, few studies have analyzed the lncRNA expression profiles of BM-MSCs, which are the main source of osteoblasts in vivo. In this report, we evaluated and analyzed lncRNA expression profiles during the osteogenic differentiation of human BM-MSCs. Thus, our research is more likely to reveal the physiological mechanisms of lncRNAs in BM-MSC osteogenesis. Moreover, we identified an uncharacterized novel osteogenesis-enriched lncRNA (named lncRNA-OG), which promoted BM-MSC osteogenesis. Additionally, unlike previous lncRNAs found in the MSC cytoplasm, such as H19, MIR31HG, and lncRNA-POIR, lncRNA-OG is mainly located in the MSC nucleus, indicating that it may regulate downstream genes at the transcriptional level. Therefore, our study identified a novel functional osteogenesis-associated lncRNA, which may be a potential and valuable target for clinical applications.

As a member of the hnRNP family, hnRNPK comprises three K homology (KH) domains that can bind to DNA or RNA and is known to regulate transcription and protein translation by directly or indirectly binding chromatin-modifying complexes [30–32]. Preliminary studies have reported that hnRNPK and other members of the hnRNP family interact with multiple lncRNAs, such as lincRNA-p21 [33], lnc-THRIL [14], and MALAT-1 [34]. LncRNAs mediate transcriptional regulation through physical associations with hnRNP family proteins. Similarly, in our study, we found that lncRNA-OG specifically associated with hnRNPK and that both molecules were co-expressed in the nucleus of BM-MSCs. A series of truncation fragments was constructed, and exon 4 of lncRNA-OG was shown to be sufficient for the formation of a complex with hnRNPK. The structure of exon 4 was predicted to form a stable stem-loop, which reportedly has a high binding affinity for associated proteins [35]. Hence, we suggest that lncRNA-OG strictly interacts with hnRNPK. Some lncRNAs, such as CASC11 and pancEts-1, bind to hnRNPK, resulting in β-catenin stabilization and transactivation [16, 36]. These studies suggest that hnRNPK directly stabilizes the lncRNA structure, so that lncRNA binding to other key proteins is more stable. We suggest that hnRNPK interacts with lncRNA-OG and stabilizes its molecular structure, which promotes the osteogenic differentiation of BM-MSCs.

Osteoblast differentiation is regulated by multiple genes and signaling pathways, such as the BMP, WNT and MAPK signaling pathways [20]. In our study, lncRNA-OG mainly regulates BMP signaling, which promotes BM-MSC osteogenesis. BMP signaling is mainly initiated by BMP family proteins, which bind to receptor complexes and activate SMAD phosphorylation [37]. Previously, lncRNA MEG3 was reported to activate BMP4 transcriptional activity *in trans* to promote MSC osteogenesis [27]. Similarly, in our study, we found that lncRNA-OG positively regulates multiple BMP family proteins. However, it is notable that lncRNA-OG regulates the expression of multiple BMP family proteins rather than a single protein. HnRNPK is known to associate with lncRNA to activate or repress gene expression by interacting with other complexes [38]. In our study, we found that a physical interaction between lncRNA-OG and hnRNPK was likely required for lncRNA-OG-mediated gene regulation because hnRNPK knockdown abrogated lncRNA-OG-enhanced BM-MSC osteogenesis and led to inhibition of the same genes. Thus, we suggest that lncRNA-OG regulates BMP family proteins by interacting with hnRNPK. Nevertheless, the precise mechanism by which lncRNA-OG regulates BMP family proteins in combination with hnRNPK remains unclear.

A variety of mechanisms have been reported to be involved in the upstream regulation of lncRNAs, such as chromosome deletion [39], transcriptional regulation by transcription factors or epigenetics [40, 41], and post-transcriptional destabilization [42]. In our study, we observed high H3K27ac enrichment at the lncRNA-OG promoter according to the UCSC database, and we demonstrated that H3K27 acetylation activated the expression of lncRNA-OG during osteogenic differentiation. Similarly, lncRNAs such as CCAT1 [43] and CASC11 [36] are upregulated because of H3K27ac activation at their promoters. In contrast, histone deacetylation results in the repression of lncRNAs [44]. Therefore, our study indicates that histone acetylation plays an important role in the upstream regulation of lncRNAs. Interestingly, our data showed that hnRNPK knockdown resulted in notable repression of lncRNA-OG transcriptional activity. HnRNPK was reported to associate with epigenetic proteins, which facilitate histone modification or DNA methylation [33, 45]. Our experiments showed that hnRNPK increased lncRNA-OG promoter H3K27 acetylation to promote lncRNA-OG transcriptional activity. Although preliminary studies reported that hnRNPK regulates gene expression through an epigenetic mechanism [30–32], few studies have shown that hnRNPK also epigenetically regulates lncRNA transcription. Therefore, based on our research, we propose a new mechanism for hnRNPK involving dual-phase action. During BM-MSC osteogenesis, hnRNPK is upregulated and promotes the expression of lncRNA-OG through H3K27ac. Moreover, hnRNPK interacts with lncRNA-OG exon 4 to promote the expression of downstream BMP family proteins, inducing the osteogenic differentiation of MSCs. Our study proposes a new and interesting phenomenon in which lncRNA-OG promotes the osteogenic differentiation of BM-MSCs by associating with hnRNPK, while the latter reciprocally regulates lncRNA-OG transcriptional activity. However, further research is required to determine whether these activities occur simultaneously or in succession.

Conclusion

In summary, we identified a novel lncRNA, named lncRNA-OG, that plays a significant, positive role in BM-MSC osteogenic differentiation by regulating the expression of BMP family proteins. H3K27 acetylation-activated lncRNA-OG was associated with hnRNPK, which simultaneously mediated lncRNA-OG transcriptional activity. This study reveals a novel lncRNA in BM-MSC osteogenesis and provides new insight into the relationship between hnRNPK and lncRNA. However, this study had limitation. Specifically, the mechanism by which lncRNA-OG interacts with hnRNPK to regulate downstream genes is unclear, which will be resolved in future research studies.

Acknowledgments

This study was supported by the National Natural Science Foundation of China (81672097, 81702120), the Industrial Technology Research and Development Funding Project of Guangdong Province (20160911) and the Clinical Medicine Research and Transformation Project of Guangzhou City (201604020004).

Author Contributions

S.T.: conception and design, collection of data, manuscript writing; Z.X.: conception and design, collection of data, data analysis and interpretation; P.W.: conception and design, data analysis and interpretation; J.L.: collection of data, data analysis; S.W.: provision of study material; W.J.: collection and assembly of data; M.L.: collection of data, data analysis and interpretation; X.W.: provision of study material, collection of data; H.S.: provision of study material; S.C., G.Y, G.Z.: collection of data; Y.W.: financial support, administrative support, final approval of manuscript; H.S.: conception and design, financial support, final approval of manuscript.

Disclosure of Potential Conflicts of Interest

The authors indicated no potential conflicts of interest.

References

1 Olsen BR, Reginato AM, Wang W. Bone development. Annu Rev Cell Dev Biol 2000; 16:191–220.
2 Kronenberg HM. Developmental regulation of the growth plate. Nature 2003;423: 332–336.
3 Grayson WL, Bunnell BA, Martin E et al. Stromal cells and stem cells in clinical bone regeneration. Nat Rev Endocrinol 2015; 11:140–150.
4 Xie Z, Wang P, Li Y et al. Imbalance between bone morphogenetic protein 2 and noggin induces abnormal osteogenic differentiation of mesenchymal stem cells in ankylosing spondylitis. Arthritis Rheumatol 2016;68: 430–440.
5 Lian WS, Wu RW, Lee MS et al. Subchondral mesenchymal stem cells from osteoarthritic knees display high osteogenic differentiation capacity through microRNA-29a regulation of HDAC4. J Mol Med 2017;95:1327–1340.
6 Wang KC, Chang HY. Molecular mechanisms of long noncoding RNAs. Mol Cell 2011;43:904–914.
7 Ulitsky I, Bartel DP. LincRNAs: Genomics, evolution, and mechanisms. Cell 2013;154: 26–46.
8 Batista PJ, Chang HY. Long noncoding RNAs: Cellular address codes in development and disease. Cell 2013;152:1298–1307.
9 Cech TR, Steitz JA. The noncoding RNA revolution-trashing old rules to forge new ones. Cell 2014;157:77–94.
10 Ramos AD, Andersen RE, Liu SJ et al. The long noncoding RNA Pnky regulates neuronal differentiation of embryonic and postnatal neural stem cells. Cell Stem Cell 2015;16: 439–447.
11 Xie Z, Li J, Wang P et al. Differential expression profiles of long noncoding RNA and mRNA of osteogenically differentiated mesenchymal stem cells in ankylosing spondylitis. J Rheumatol 2016;43:1523–1531.
12 Klimek-Tomczak K, Wyrwicz LS, Jain S et al. Characterization of hnRNP K protein-RNA interactions. J Mol Biol 2004;342:1131–1141.
13 Bomsztyk K, Denisenko O, Ostrowski J. HnRNP K: One protein multiple processes. BioEssays 2004;26:629–638.
14 Li Z, Chao TC, Chang KY et al. The long noncoding RNA THRIL regulates TNFalpha expression through its interaction with hnRNPL. Proc Natl Acad Sci USA 2014;111: 1002–1007.
15 Huarte M, Guttman M, Feldser D et al. A large intergenic noncoding RNA induced by p53 mediates global gene repression in the p53 response. Cell 2010;142:409–419.
16 Li D, Wang X, Mei H et al. Long noncoding RNA pancEts-1 promotes neuroblastoma progression through hnRNPK-mediated beta-catenin stabilization. Cancer Res 2018;78: 1169–1183.
17 Xie Z, Tang S, Ye G et al. Interleukin-6/interleukin-6 receptor complex promotes osteogenic differentiation of bone marrow-derived mesenchymal stem cells. Stem Cell Res Ther 2018;9:13.
18 Xie Z, Wang P, Li J et al. MCP1 triggers monocyte dysfunctions during abnormal osteogenic differentiation of mesenchymal stem cells in ankylosing spondylitis. J Mol Med 2017;95:143–154.
19 Dominici M, Le Blanc K, Mueller I et al. Minimal criteria for defining multipotent mesenchymal stromal cells. The International Society for Cellular Therapy position statement. Cytotherapy 2006;8:315–317.
20 Long F. Building strong bones: Molecular regulation of the osteoblast lineage. Nat Rev Mol Cell Biol 2011;13:27–38.
21 Pittenger MF, Mackay AM, Beck SC et al. Multilineage potential of adult human mesenchymal stem cells. Science 1999;284: 143–147.
22 Liu X, Kumagai G, Wada K et al. Suppression of osteogenic differentiation in mesenchymal stem cells from patients with ossification of the posterior longitudinal ligament by a histamine-2-receptor antagonist. Eur J Pharmacol 2017;810:156–162.
23 Ng SY, Bogu GK, Soh BS et al. The long noncoding RNA RMST interacts with SOX2 to regulate neurogenesis. Mol Cell 2013;51: 349–359.
24 Xiao T, Liu L, Li H et al. Long noncoding RNA ADINR regulates adipogenesis by transcriptionally activating C/EBPalpha. Stem Cell Rep 2015;5:856–865.
25 Carlson HL, Quinn JJ, Yang YW et al. LncRNA-HIT functions as an epigenetic regulator of chondrogenesis through its recruitment of p100/CBP complexes. PLoS Genet 2015;11:e1005680.
26 Huang Y, Zheng Y, Jia L et al. Long noncoding RNA H19 promotes osteoblast differentiation via TGF-beta1/Smad3/HDAC signaling pathway by deriving miR-675. Stem Cells 2015; 33:3481–3492.
27 Zhuang W, Ge X, Yang S et al. Upregulation of lncRNA MEG3 promotes osteogenic differentiation of mesenchymal stem cells from multiple myeloma patients by targeting BMP4 transcription. Stem Cells 2015; 33:1985–1997.
28 Jin C, Jia L, Huang Y et al. Inhibition of lncRNA MIR31HG promotes osteogenic differentiation of human adipose-derived stem cells. Stem Cells 2016;34:2707–2720.
29 Wang L, Wu F, Song Y et al. Long noncoding RNA related to periodontitis interacts with miR-182 to upregulate osteogenic differentiation in periodontal mesenchymal stem cells of periodontitis patients. Cell Death Dis 2016;7:e2327.
30 Ritchie SA, Pasha MK, Batten DJ et al. Identification of the SRC pyrimidine-binding protein (SPy) as hnRNP K: Implications in the regulation of SRC1A transcription. Nucl Acids Res 2003;31:1502–1513.
31 Lau JS, Baumeister P, Kim E et al. Heterogeneous nuclear ribonucleoproteins as regulators of gene expression through interactions with the human thymidine kinase promoter. J Cell Biochem 2000;79:395–406.
32 Lynch M, Chen L, Ravitz MJ et al. HnRNP K binds a core polypyrimidine element in the eukaryotic translation initiation factor 4E (eIF4E) promoter, and its regulation of eIF4E contributes to neoplastic transformation. Mol Cell Biol 2005;25:6436–6453.
33 Bao X, Wu H, Zhu X et al. The p53-induced lincRNA-p21 derails somatic cell reprogramming by sustaining H3K9me3 and CpG methylation at pluripotency gene promoters. Cell Res 2015;25:80–92.
34 Yang F, Yi F, Han X et al. MALAT-1 interacts with hnRNP C in cell cycle regulation. FEBS Lett 2013;587:3175–3181.
35 Wang Y, He L, Du Y et al. The long noncoding RNA lncTCF7 promotes self-renewal of human liver cancer stem cells through activation of Wnt signaling. Cell Stem Cell 2015;16:413–425.
36 Zhang Z, Zhou C, Chang Y et al. Long noncoding RNA CASC11 interacts with hnRNP-K and activates the WNT/beta-catenin pathway to promote growth and metastasis in colorectal cancer. Cancer Lett 2016;376:62–73.

37 Feng XH, Derynck R. Specificity and versatility in tgf-beta signaling through Smads. Annu Rev Cell Dev Biol 2005;21: 659–693.
38 Kim K, Choi J, Heo K et al. Isolation and characterization of a novel H1.2 complex that acts as a repressor of p53-mediated transcription. J Biol Chem 2008;283:9113–9126.
39 Zhang J, Li Z, Liu L et al. Long noncoding RNA TSLNC8 is a tumor suppressor that inactivates the interleukin-6/STAT3 signaling pathway. Hepatology 2018;67:171–187.
40 Xie JJ, Jiang YY, Jiang Y et al. Increased expression of the long non-coding RNA LINC01503, regulated by TP63, in squamous cell carcinoma and effects on oncogenic activities of cancer cell lines. Gastroenterology 2018;154:2137.e1–2151.e1.
41 Hadji F, Boulanger MC, Guay SP et al. Altered DNA methylation of long noncoding RNA H19 in calcific aortic valve disease promotes mineralization by silencing NOTCH1. Circulation 2016;134:1848–1862.
42 Hammerle M, Gutschner T, Uckelmann H et al. Posttranscriptional destabilization of the liver-specific long noncoding RNA HULC by the IGF2 mRNA-binding protein 1 (IGF2BP1). Hepatology 2013;58:1703–1712.
43 Zhang E, Han L, Yin D et al. H3K27 acetylation activated-long non-coding RNA CCAT1 affects cell proliferation and migration by regulating SPRY4 and HOXB13 expression in esophageal squamous cell carcinoma. Nucl Acids Res 2017;45:3086–3101.
44 Yang F, Huo XS, Yuan SX et al. Repression of the long noncoding RNA-LET by histone deacetylase 3 contributes to hypoxia-mediated metastasis. Mol Cell 2013;49: 1083–1096.
45 Chu C, Zhang QC, da Rocha ST et al. Systematic discovery of Xist RNA binding proteins. Cell 2015;161:404–416.


See www.StemCells.com for supporting information available online.